

Electronic Supporting Information

Ferrocenyl-terminated polyphenylene-type dendrimers as supports for gold and palladium nanocatalysis

Wenjuan Wang,^{a,b} Elena S. Serkova^c, Eduardo Guisasola Cal,^d Desire Di Silvio,^e Marta Martínez Moro,^d Sergio Moya,^d Jean-René Hamon,^b Didier Astruc^{a,*} and Zinaida B. Shifrina^{c,*}

a. ISM, UMR CNRS 5255, Université de Bordeaux, Talence 33405 Cedex, France. E-mail: didier.astruc@u-bordeaux.fr

b. Institut des Sciences Chimiques, UMR CNRS 6226, Université de Rennes 1, 35042 Rennes Cedex, France.

c. A.N. Nesmeyanov Institute of Organoelement Compounds of Russian Academy of Sciences, Moscow 119991, Russia.

E-mail: z_shifrina@yahoo.com

d. Soft Matter Nanotechnology Lab, CIC biomaGUNE, Paseo Miramón 182, 20014 Donostia-San Sebastián, Gipuzkoa, Spain.

e. Surface Analysis and Fabrication Platform Manager, Parque Científico y Tecnológico de Gipuzkoa, Paseo Miramón 194, 20014 Donostia / San Sebastián · Gipuzkoa · Spain.

Table of contents

	page
1. General data	1
2. The XPS data of Fe 2p in FcMTD alone, Pd(II)-FcMTPD and Pd(0) NP@FcMTPD.	1-3
3. UV-vis. spectrum of FcMTD -stabilized PdNPs-1 and PdNPs-2.	4
4. The method for calculation of the determination of the apparent rate constant k_{app} for the 4-nitrophenol reduction reaction	4
5. TEM images and size distribution histogram of MNP-1 after the 1 st cycle	5-6
6. TEM images and size distribution histogram of MNPs-1 and their UV-vis. spectrum after the 1 st cycle	7
7. Calculation of the NP surface atoms number (N_s), total surface (S) and $k_0 = k_{app}/S$ related to the NPs for the 4-nitrophenol reduction reaction.	8

1. General data

All the solvents and chemicals were used as received. ^1H NMR spectra were recorded at 25 °C with a Bruker AC 300 MHz. All the chemical shifts are reported in parts per million (δ , ppm) with reference to Me_4Si in CDCl_3 . Transmission Electron Microscopy (TEM): The sizes of the MNPs were determined by TEM using a JEOL JEM 1400 (120 kV) microscope. The TEM samples were prepared by deposition of the nanoparticle suspension (10 μL) onto a carbon-coated microscopy copper grid. X-ray Photoelectron Spectroscopy (XPS): System: SPECS SAGE HR; X-Ray source: Al K α non-monochromatic; operated at 12.5 kV and 300 W. Take off angle 90°, at $\sim 10^{-8}$ Torr. Pass energy for survey spectra 30 eV, 10 eV for narrow scans analysis; spectra are calibrated to C-C carbon 285 eV. Analysis is consisted of Shirley background subtraction. Peaks are fitted with symmetrical Gaussian-Lorentzian (GL) line shapes. Samples are prepared by dehydration on the titania coated glass or silica substrates. Titania is selected as a substrate to avoid the overlap of Si and Au. Flash column chromatography was performed using silica gel (300-400 mesh).

2. The XPS data of Fe 2p in FcMTD alone, Pd(II)-FcMTPD and Pd(0) NP@FcMTPD.

Table S1 The XPS data of Fe 2p in FcMTD alone, Pd(II)-FcMTPD and Pd(0) NP@FcMTPD.

	Fe II 2p_{3/2} BE(eV) [at%]	Fe III 2p_{3/2} BE(eV) [at%]
FcMTD	707.9 [100]	-
FcMTD + Pd²⁺	707.8 [64]	709.8 [36]
FcMTD -PdNPs	707.7 [100]	-

Fe 2p in FcMTD sample showed the typical spectrum for ferrocene with two satellites. In FcMTD + Pd²⁺ three peaks appeared (2p 3/2 709.8 eV, 2p 1/2 722.9 eV, satellite 730.6 eV) that are compatible with Fe(III).^{4,5} Fe 2p in FcMTD -PdNPs sample showed the typical spectrum for ferrocene, but the high S/N does not allow to appreciate the two satellites at about 711eV and 718 eV.

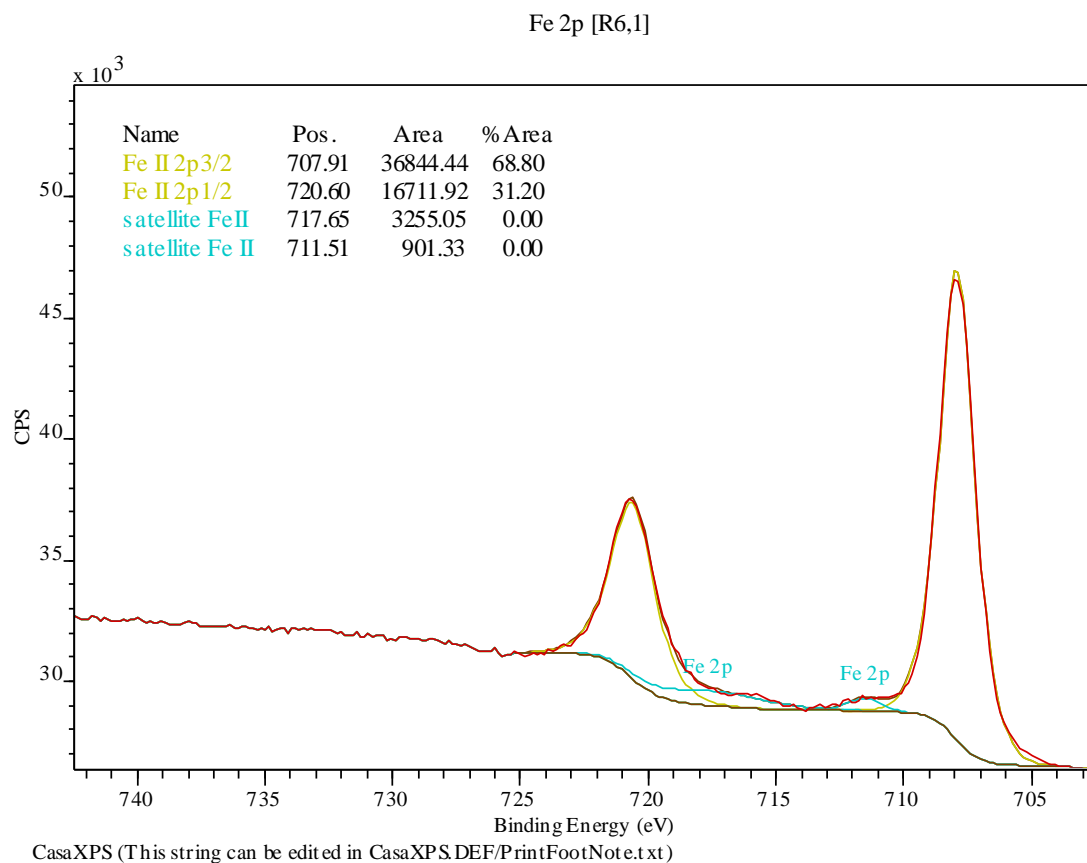


Fig. S1. XPS spectra of Fe 2p in the sample FcMTD alone.

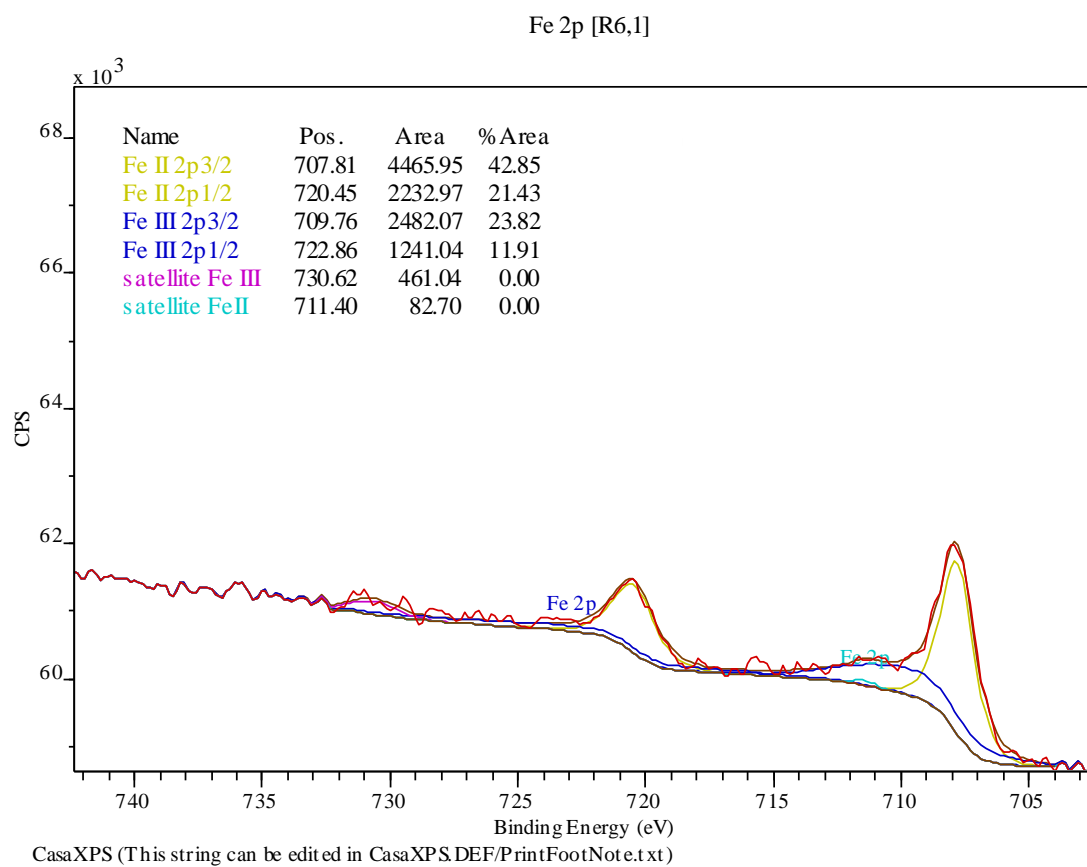


Fig. S2. XPS spectra of Fe 2p in the sample Pd(II)-FcMTPD.

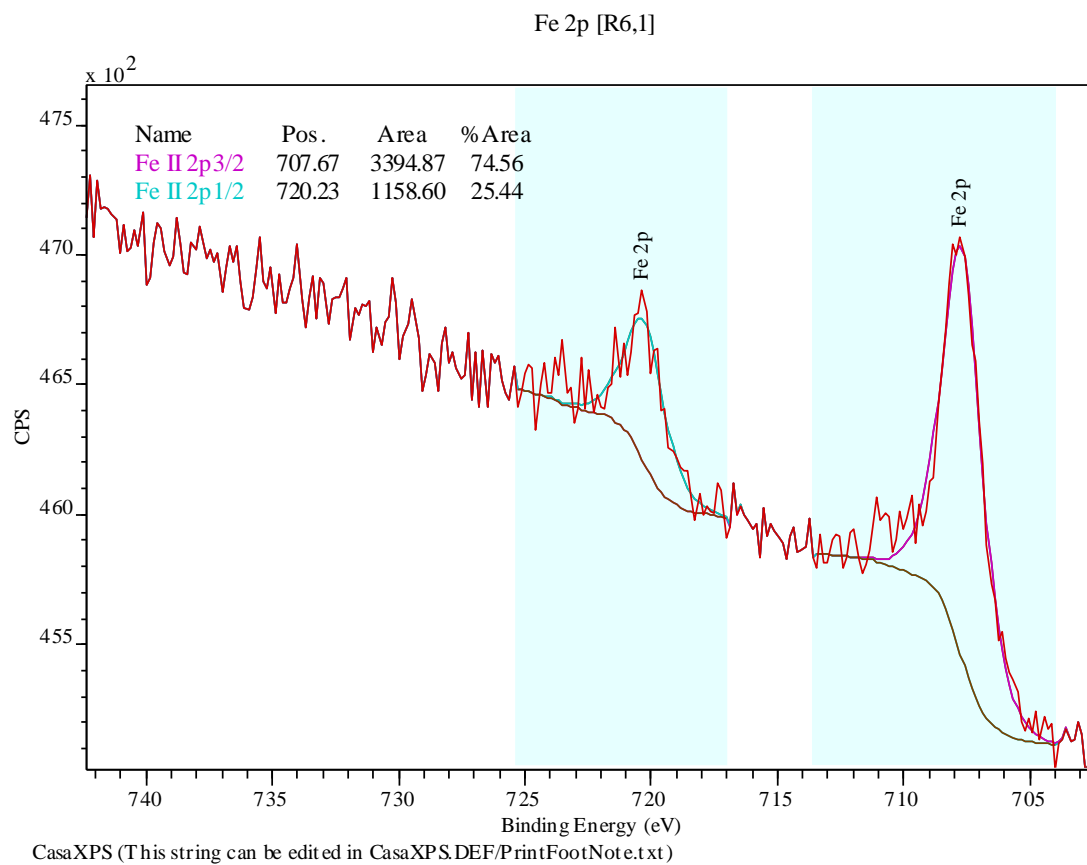


Fig. S3. XPS spectra of Fe 2p in the sample Pd(0) NP@FcMTPD.

3. UV-vis. spectrum of FcMTD-stabilized PdNPs-1 and PdNPs-2

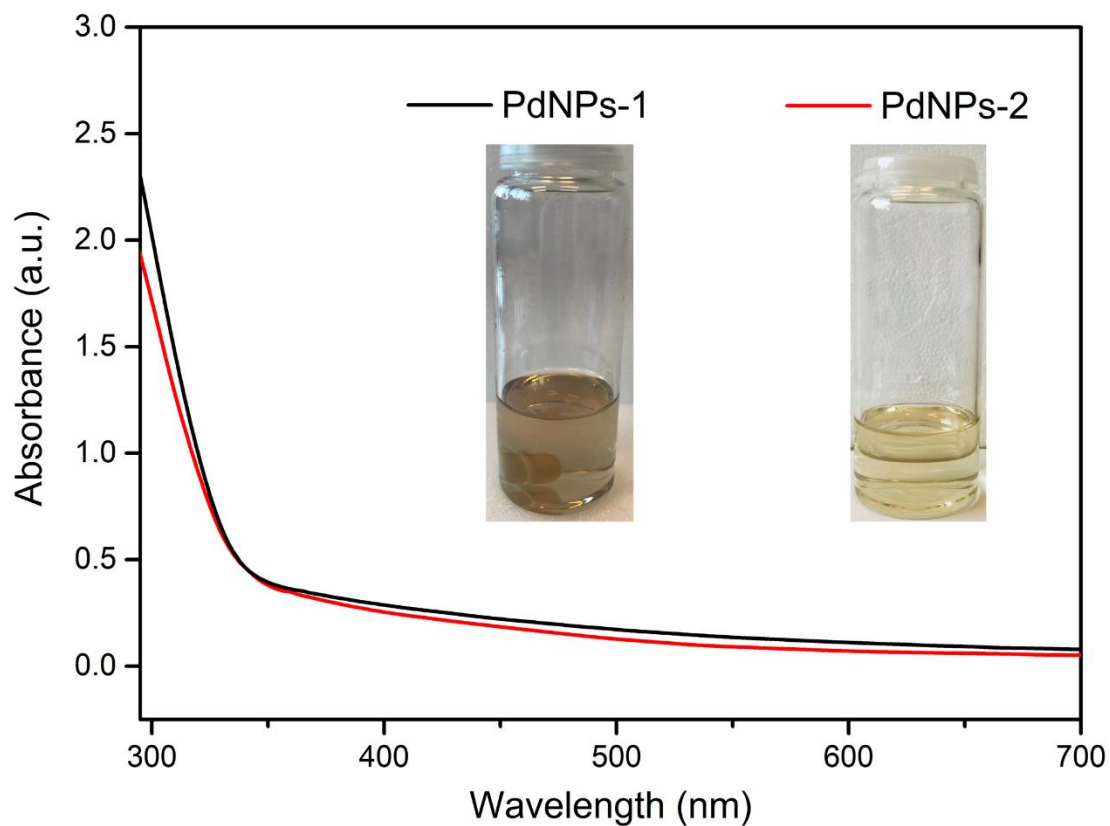


Fig. S4 UV-vis. spectrum of FcMTD -stabilized PdNPs-1 and PdNPs-2. Insert: the photograph of PdNPs-1 (left) and PdNPs-2 (right).

4. Determination of the rate constant k_{app} of the 4-nitrophenol reduction reaction

The reaction is fitted with a pseudo-first-order kinetics with respect to 4-NP in the presence of excess NaBH_4 , leading to the determination of the rate constant k_{app} (eqn (1)):

$$-\ln(C_t/C_0) = k_{app}t \quad (1)$$

(C_t is the concentration of 4-NP at a time t , and C_0 is the concentration of 4-NP at time $t = 0$).

5. Synthesis of the MNPs-3 stabilized by FcMTPD.

FcMTPD was prepared according to the literature procedure by copper-catalyzed azide-alkyne cycloaddition (CuAAC) reaction between a previously reported ethynyl-terminated dendrimer and azidomethylferrocene. Then, a solution ($V_{\text{CH}_2\text{Cl}_2}/V_{\text{MeOH}} = 30:1$, 6.8 mL) of Na_2PdCl_4 (or HAuCl_4 , 1.0×10^{-3} mmol, $n_{\text{metal}}: n(\text{Triazole} + \text{Pyridine}) = 1:1$) was mixed with a solution ($V_{\text{CH}_2\text{Cl}_2}/V_{\text{methanol}} = 30:1$, 3 mL) of the dendrimer FcMTPD (2.5×10^{-5} mmol) in a 20 mL flask with a stir bar. After the mixture was stirred for 30 min, then 5.0×10^{-3} mmol of NaBH_4 was added into the flask under vigorous stirring. After continuous stirring for 1 h at room temperature, the metal nanoparticles were obtained.

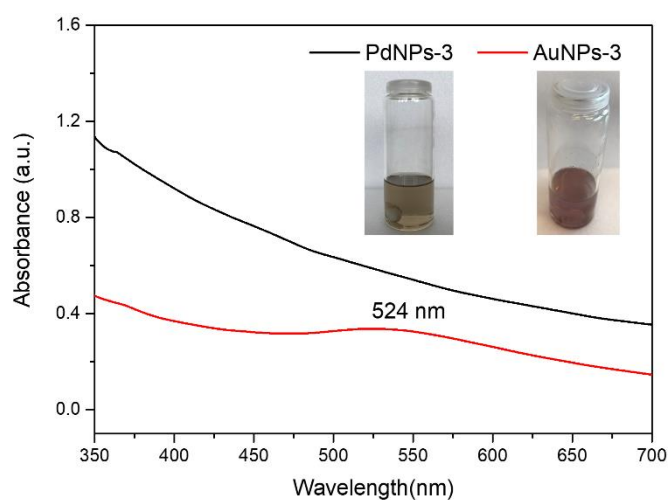


Fig. S5 UV-vis. spectrum of FcMTPD-stabilized PdNPs-3 and AuNPs-3. Insert: the photograph of PdNPs-3 (left) and AuNPs-3 (right).

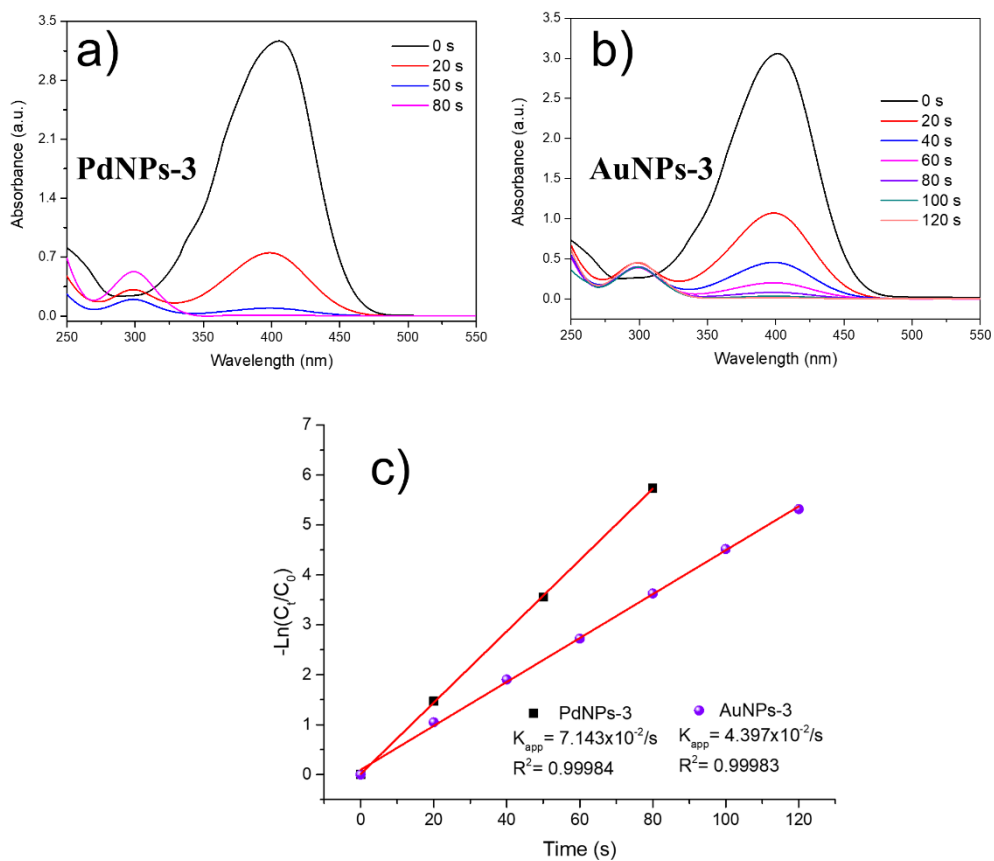


Fig. S6. Time-dependent UV-vis. spectrum of the *p*-nitrophenol reduction reaction in the presence of 0.5% mmol of PdNPs-3 (a) and AuNPs-3 (b). (c) Plots of the consumption rate of 4-NP: $[-\ln(C_t/C_0)]$ vs. reaction time with 0.5% mmol of MNPs-3.

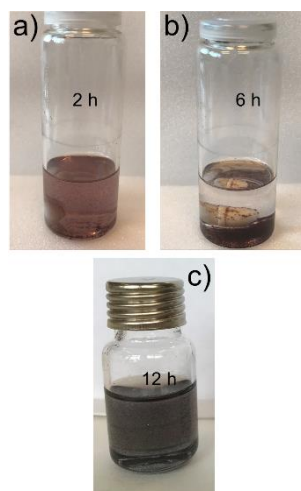


Fig. S7. The photograph of AuNPs-3 (a, b) and PdNPs-3 (c).

6. TEM images and size distribution histogram of MNPs-1 and their UV-vis. spectrum after the 1st cycle

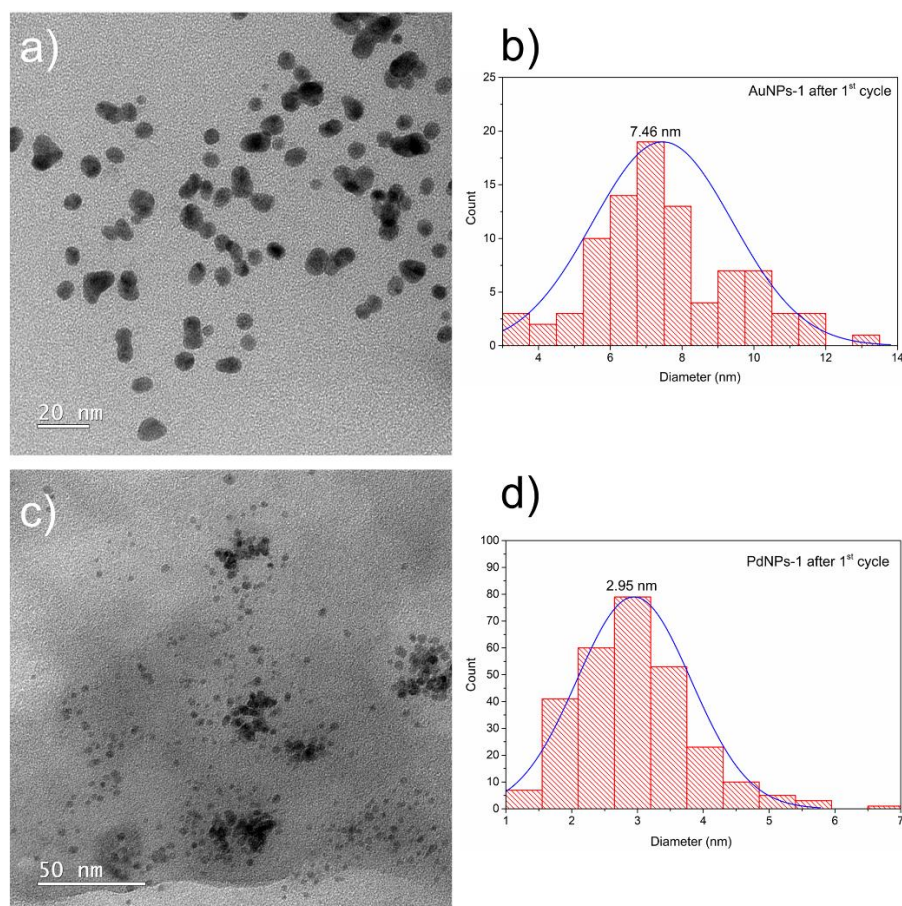


Fig. S8. TEM images of PdNPs-1 (a) and AuNPs-1 (c) after the 1st cycle; size distribution histogram of PdNPs-1 (b) and AuNPs-1 (d) after 1st the cycle.

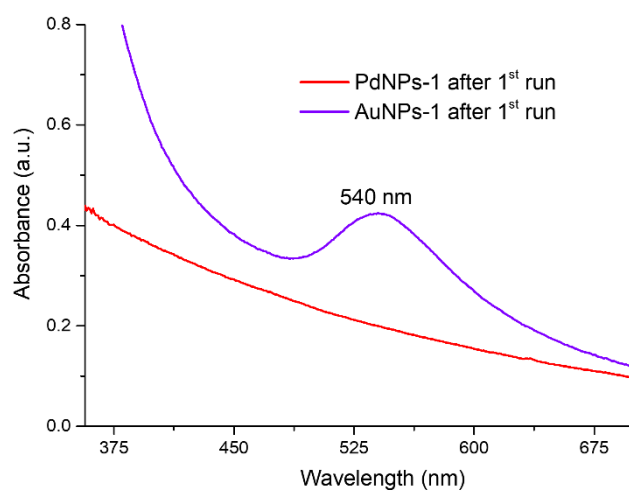


Fig. S9 UV-vis. spectrum of FcMTD-stabilized PdNPs-1 and AuNPs-1 after 1st run.

7. Calculation of the NP surface atoms number (Ns) and k_0 related to the Ns.

$$V_{NP} = NV_{atom} \text{ (eq. 1)}$$

$$4/3\pi(R_{NP})^3 = N 4/3\pi(R_{atom})^3 \text{ (eq. 2)}$$

Where V is the atom volume of the NP, R is the atomic radius of the NP, and N is the total number of atoms within the NP. Rearranging, we obtain:

$$N = (R_{NP}/R_{atom})^3 \text{ (eq. 3)}$$

Knowing the NP radius, we can also calculate the surface area of a NP with the following equation:

$$S_{NP} = 4\pi(R_{NP})^2 \text{ (eq. 4)}$$

$$N'_{NP} = (N_M/N) \times 6.02 \times 10^{23} \text{ (eq. 5)}$$

$$S = S_{NP} N'_{NP} \text{ (eq. 6)}$$

Normalized to the unit volume of the system, where N'_{NP} is the total number of metal nanoparticles, S is total surface area of metal nanoparticles, N_M is the molar of metal nanoparticles.

$$k_{app} = k_0 S \text{ (eq. 7)}^1$$

Table S2. Physical properties and catalytic efficiencies of the nanocatalysts.

	R_{atom}^a (nm)	R_{NP}^b (nm)	k_{app}^c ($10^{-2} s^{-1}$)	$k_0^{d,e}$ [$s^{-1}m^{-2}L$]	[N_M] [mmol/L]	$S^{d,f}$ [m^2/L]
PdNPs-1	0.137	1.0	7.80	0.348	1.15×10^{-2}	0.224
AuNPs-1	0.144	1.8	5.59	0.386		0.145
PdNPs-2	0.137	1.85	3.95	0.326		0.12
AuNPs-2	0.144	3.25	0.95	0.119		0.08

^a Radius of the metal atomic. ^b Radius of the metal particles. ^c Apparent rate constant. ^d Calculated from the data given in the respective papers. ^e Rate constant normalized to the surface of the particles in the system (eq 7). ^f Surface area of metal nanoparticles normalized to the unit volume of the system.

Reference

1. Y. Mei, G. Sharma, Y. Lu and M. Ballauff, *Langmuir*, 2005, **21**, 12229-12234.